Involvement of TRPV2 and SOCE in calcium influx disorder in DMD primary human myotubes with a specific contribution of α 1 -syntrophin and PLC/PKC in SOCE regulation

Rania Harisseh, Aurélien Chatelier, Christophe Magaud, Nadine Déliot, Bruno Constantin

Am J Physiol Cell Physiol 304: C881–C894, 2013.
First published February 20, 2013; doi:10.1152/ajpcell.00182.2012.

Involvement of TRPV2 and SOCE in calcium influx disorder in DMD primary human myotubes with a specific contribution of α_1-syntrophin and PLC/PKC in SOCE regulation

Rania Harisseh, Aurélien Chatelier, Christophe Magaud, Nadine Déliot, and Bruno Constantin

Institut de Physiologie et Biologie Cellulaires, Université de Poitiers/Centre National de la Recherche Scientifique FRE-3511 Poitiers, France

Submitted 30 May 2012; accepted in final form 18 February 2013

Harisseh R, Chatelier A, Magaud C, Déliot N, Constantin B. Involvement of TRPV2 and SOCE in calcium influx disorder in DMD primary human myotubes with a specific contribution of α_1-syntrophin and PLC/PKC in SOCE regulation. *Am J Physiol Cell Physiol* 304: C881–C894, 2013. First published February 20, 2013; doi:10.1152/ajpcell.00182.2012.—Calcium homeostasis is critical for several vital functions in excitable and nonexcitable cells and has been shown to be impaired in many pathologies including Duchenne muscular dystrophy (DMD). Various studies using murine models showed the implication of calcium entry in the dystrophic phenotype. However, alteration of store-operated calcium entry (SOCE) and transient receptor potential vanilloid 2 (TRPV2)-dependant cation entry has not been investigated yet in human skeletal muscle cells. We pharmacologically characterized basal and store-operated cation entries in primary cultures of myotubes prepared from muscle of normal and DMD patients and found, for the first time, an increased SOCE in DMD myotubes. Moreover, this increase cannot be explained by an over expression of the well-known SOCE actors: TRPC1/4, Orai1, and stromal interaction molecule 1 (STIM1) mRNA and proteins. Thus we investigated the modes of regulation of this cation entry. We firstly demonstrated the important role of the scaffolding protein α_1-syntrophin, which regulates SOCE in primary human myotubes through its PDZ domain. We also studied the implication of phospholipase C (PLC) and protein kinase C (PKC) in SOCE and showed that their inhibition restores normal levels of SOCE in DMD human myotubes. In addition, the involvement of TRPV2 in calcium deregulation in DMD human myotubes was explored. We showed an abnormal elevation of TRPV2-dependant cation entry in dystrophic primary human myotubes compared with normal ones. These findings show that calcium homeostasis mishandling in DMD myotubes depends on SOCE under the influence of Ca^{2+}/PLC/PKC pathway and α_1-syntrophin regulation as well as on TRPV2-dependant cation influx.

DMD; human primary myotubes; Ca^{2+}/PLC/PKC; α_1-syntrophin; TRPV2; SOCE

CALCIUM HOMEOSTASIS IS BASED on strictly cohesive and regulated communication between internal and plasma membrane calcium channels and pumps and has been shown to be altered in several pathologies and particularly in dystrophinopathies including Duchenne muscular dystrophy (DMD; Ref. 5). DMD is characterized by an abnormally high concentration of intracellular ionized calcium (7), which is thought to contribute to the final muscle necrosis. DMD is an X-linked recessive genetic disorder that affects 1 male birth over 3,500 in the world. This disease is caused by mutations on the locus Xp21.2 of the gene encoding the subsarcolemmal dystrophin, resulting in the loss of this protein (57). In the absence of dystrophin, the transmembrane dystrophin glycoprotein complex components lose their localization at costamers. This disorganization is thought to be responsible for membrane instability and muscle damage and for alterations in cell signaling and calcium homeostasis (4).

Impairment of calcium homeostasis in DMD has been largely investigated in mouse myotubes and fibers. Several studies characterized abnormal calcium entry in dystrophin-deficient skeletal muscle cells attributed to deregulated sarcolemmal calcium permeable channels (17, 23, 56). Calcium influx through transient receptor potential canonical (TRPC) channels has even been shown to be sufficient to induce muscular dystrophy in vivo in a study on transgenic mice overexpressing TRPC3 (42). Moreover, stretch-activated channels (SAC) have been studied by the cell-attached patch-clamp technique and displayed an increased open probability and occurrence in *mdx* myotubes (a commonly used DMD mouse model; Refs. 18, 19) and in human DMD myotubes (60). In a study on *mdx* fibers, enhanced activity of store-operated channels was described with similar characteristics than SAC recorded in the same preparation (13). TRP vanilloid 2 (TRPV2), a cationic channel with mechanosensitivity (44), has been particularly studied in dystrophin-deficient skeletal muscle cells. TRPV2 is normally localized in intracellular membrane compartments, but its translocation to the plasma membrane is increased in dystrophic muscle fibers (28). Its specific inhibition appears to improve muscular dystrophy. Indeed, *mdx* mice expressing a dominant-negative TRPV2 have a reduced Ca^{2+} entry in their muscle fibers. This TRPV2 mutant also displays reduced muscle degeneration (necrosis and apoptosis) and regeneration (central nuclei, etc.). These observations suggest that the TRPV2 channel is an important pathway of Ca^{2+} entry in dystrophic muscle (29, 64).

Our group also showed an abnormal increase in store-operated calcium entry (SOCE) in dystrophin-deficient mouse myotubes corrected by a stable tranfection with minidystrophin (41, 58). The regulation of SOCE involves the subsarcolemmal scaffolding protein α_1-syntrophin, which is capable of correcting the abnormal increase of SOCE in dystrophin-deficient mouse myotubes (50, 59). The identity and regulation of SOCE are now better understood but still a matter of debate and several proteins seem to participate to SOCE. Different studies have pointed out the implication of TRPC channels (50, 59, 61) of stromal interaction molecule 1 (STIM1; Refs. 38, 48) and of Orai1, the protein responsible for CRAC currents (40, 62) in the mechanism of calcium entry triggered by sarcoplasmic reticulum (SR) Ca^{2+} store depletion in skeletal muscle.

Address for reprint requests and other correspondence: B. Constantin, Institut de Physiologie et Biologie Cellulaires, Université de Poitiers/CNRS FRE-3511, 86022 Poitiers Cedex, France (e-mail: bruno.constantin@univ-poitiers.fr).

In human skeletal muscle cells, dysfunctional calcium handling was also documented in particular altered calcium influx. The regulation of the free cytosolic calcium concentration is known to be impaired in DMD human myotubes (17), and studies using contracting myotubes suggested that the calcium elevation resulted from abnormal activation of cation channels or from membrane alteration during contraction (24–26). Moreover, in DMD myotubes, stretch-activated channels are known to be abnormally stimulated (60), and although calcium entry through the reverse mode of Na^+/Ca^{2+} exchanger was unchanged, the resulting calcium-induced calcium release was increased (12). Other alternative pathways for calcium entry were described in human myotubes such as SOCE, which has been evoked in normal human myotubes by activation of ryanodine receptors (RyR; Ref. 63). SOCE has also been described in resealed T-tubular systems of skinned fibers from malignant hypothermia patients (14) and shown to be dependent on STIM1 (48). However, most of calcium mishandling mechanisms have been described in the *mdx* mouse, which displays a different dystrophic phenotype than humans.

The previous work on *mdx* dystrophic mouse muscle cells suggested that calcium mishandling is preponderant in the development of dystrophic phenotype. For instance, artificially increased TRPC-dependent calcium entries were recently shown to be sufficient to induce muscular dystrophy in mouse independently on membrane fragility (42). On the other hand, expression of a dominant-negative TRPV2 mutant was shown to reduce calcium influx through inhibition of endogenous TRPV2 in FDB fibers and to ameliorate muscular dystrophy in *mdx* mouse (29). Two different calcium influx pathway through SOC or TRPV2 channels could thus be determinant for DMD physiopathology. This prompted us to characterize store-operated cation entry as well as TRPV2-dependent calcium entry of normal and DMD primary cultured human myotubes. Because of our previous findings on dystrophin- or syntrophin-deficient myotubes (49), we also studied the implication of α_1-syntrophin but also of phospholipase C (PLC) and protein kinase C (PKC) in the impairment of Ca^{2+} entry in human myotubes.

MATERIALS AND METHODS

Antibodies and Drugs

Antibodies against TRPC1, Orai1 (Sigma-Aldrich), and TRPC4 (Alomone) were rabbit polyclonal. Antibodies against STIM1 (BD Biosciences) and α-tubulin (Sigma-Aldrich) were mouse monoclonal while antibodies against TRPV2 (Santa Cruz) and α_1-syntrophin (Abcam) were goat polyclonal. Gadolinium (Gd^{3+}); 2-aminoethoxydiphenyl borate (2APB); 1{β-[3-(4-methoxyphenyl) propoxyl]-4-methoxyphenethyl}-1*H*-imidazole hydrochloride (SKF-96365); *N*,*N*,*N*′,*N*′-tetrakis(2-pyridylmethyl)ethilenediamine (TPEN); 4-methyl-4′-[3,5-bis(trifluoromethyl)-1H-pyrazol-1-yl]-1,2,3-thiadiazole-5-carboxanilide (YM-58483); nifedipine; U73122; U73343; bisindolylmaleimide I (BIM); ruthenium red (RR); cyclopiazonic acid (CPA); and caffeine were all purchased from Sigma-Aldrich. Δ^9-Tetrahydrocannabinol (THC) was kindly donated by Dr. M. Solinas.

Cell Culture

Primary myoblasts (normal and DMD) were obtained from Myobank and Myoxis (Association Française Contre la Myopathie). Cells were seeded in 6-well or 12-well plates on Matrigel-coated glass coverslips. Cells were cultured at 25,000 cells/well (6-well plates) and 12,000 cells/well (12-well plates) in growth medium (skeletal muscle cell growth medium purchased from PromoCell supplemented with a mix provided by Promocell, 15% fetal calf serum, 1% L-glutamine, and 50 μg/ml gentamicin). At confluence, growth medium was replaced by differentiation medium (97% DMEM, 2% horse serum, 1% L-glutamine, 50 μg/ml gentamicin, and 10 μg/ml insulin). Experiments were performed after 11 days of fusion, the estimated time for myotubes formation and differentiation.

Cell Transfection

Plasmid transfection. Differentiated myotubes were transfected using jetPRIME transfection reagent (Polyplus Transfection) with a 1:2 ratio (DNA μg: jetPRIME μl). For six-well plates, 8 μl of jetPRIME transfection reagent were added to a mix of 4 μg of DNA diluted in 200 μl of transfection buffer. After a 10-min incubation at room temperature, the transfection mix was added to the well drop wise onto the cells kept in regular cell growth medium. Medium was replaced after a 4-h incubation at 37°C, 5% CO_2. Experiments were performed 48 h after transfection. Normal and DMD primary human myotubes were transfected with wild-type (WT) TRPV2 and dominant-negative TRPV2 (DK; substitution of Glu594 and Glu604 with lys; Ref. 29) in pIRES2-AcGFP1 vector, kindly donated by Dr. Y. Iwata, and with full-length α_1-syntrophin (FL α_1-syn) and α_1-syntrophin without its PDZ (ΔN α_1-syn) in the pCMS-EGFP plasmid. Control transfection was performed with Pmax.

ShRNA infection. Differentiated myotubes were infected with a mixture of 5 μg/ml polybrene and PLCβ_1 or CopGFP lentiviral particules (Santa Cruz) and incubated for 24 h. Medium was then removed and replace by fresh culture medium. Experiments were performed 48 h after infection.

Western Blotting

Proteins were extracted from differentiated myotubes cultures using RIPA buffer [50 mM Tris·HCl, 100 mM NaCl, 5 mM EDTA, 0.05% NP-40, 1% DOC, 1% Triton X-100, 0.1% SDS supplemented with AEBSF and anti-protease cocktail (Sigma-Aldrich)]. Cell extract was then passed through insulin syringe and sonicated. Protein extracts were dosed using BCA kit (Sigma-Aldrich) at 562 nm and then divided into 40-μg samples and denatured by incubation in Laemmli buffer 2× (Sigma-Aldrich) for 30 min at room temperature. Samples were then subjected to SDS-PAGE and Western blot analysis. The blots were treated with primary antibody solutions overnight then for 1 h with horseradish peroxidase-conjugated secondary antibody and developed with enhanced chemiluminescence kit (Amersham). The apparent molecular weight was estimated according to the position of prestained protein markers (kaleidoscope; Bio-Rad).

Immunostaining

The cultured myotubes were fixed in TBS (20 mM Tris base, 154 mM NaCl, 2 mM EGTA, and 2 mM $MgCl_2$, pH 7.4)/4% paraformaldehyde and permeabilized with TBS/0.5% Triton X-100. Cells were then incubated overnight with primary antibodies in TBS/1% BSA (Sigma-Aldrich) and for 45 min with secondary antibodies in TBS/1% BSA. Samples were mounted using Mowiol mounting medium (Sigma-Aldrich). The immunolabeled samples were examined by confocal laser scanning microscopy using a Bio-Rad MRC 1024 ES equipped with an argon-krypton gas laser. Data were acquired using an inverted microscope (Olympus IX70) with ×60 water immersion objective [image processing was performed with Olympus Fluoview (FV10-ASW 2.0) for adjustments of brightness and contrast].

Ca^{2+} Influx Measurement Using Mn^{2+} Quenching of Fura 2 Fluorescence

Differentiated myotubes, plated on glass coverslips, were briefly rinsed with a standard external solution 1.8 mM Ca^{2+} solution (130

mM NaCl, 5.4 mM KCl, 1.8 mM $CaCl_2$, 0.8 mM $MgCl_2$, 10 mM HEPES, and 5.6 mM D-glucose, pH 7.4, with NaOH) and incubated for 45 min at 37°C, 5% CO_2 in the same solution supplemented with 3 μM (final concentration) of fura 2-AM (Santa Cruz). After being loaded, cells were washed with Ca^{2+}-free solution (130 mM NaCl, 5.4 mM KCl, 0.1 mM EGTA, 0.8 mM $MgCl_2$, 10 mM HEPES, and 5.6 mM D-glucose, pH 7.4 with NaOH) before measurement of calcium influx. Cells were perfused by means of a homemade gravity microperfusion device. Fura 2-loaded cells were excited at 360 nm with a CAIRN monochromator (Cairn Research Limited, Faversham, UK), and emission fluorescence was monitored at 510 nm using a CCD camera (Photonic Science, Robertsbridge, UK) coupled to an Olympus IX70 inverted microscope (×40 water immersion fluorescence objective). The influx of Mn^{2+} through cationic channels was evaluated by the quenching of the fura 2 fluorescence excited at 360 nm, i.e., at the isosbestic point. The variation of fluorescence was recorded with the Imaging Workbench 4.0 (IW 4.0) software (Indec BioSystems, Mountain View, CA). Cells were tested without or after a 6-min depletion protocol consisting of three times 1-min alternated application of free Ca^{2+} solution + 5 μM CPA + 10 mM caffeine and of free Ca^{2+} solution + 15 μM CPA. Cation influx was generated by perfusion of Mn^{2+} solution (130 mM NaCl, 5.4 mM KCl, 1.8 mM $CaCl_2$, 0.8 mM $MgCl_2$, 10 mM HEPES, 5.6 mM D-glucose, and 50 μM $MnCl_2$).

Ca^{2+} Measurement Data Analysis

The rate of fluorescence intensity loss at 360 nm was divided by the initial fluorescence intensity in the cell measured before manganese ions were added to correct for differences in the cell size or fura 2 loading. The quench rate, of the fluorescence intensity, expressed as percent per minute, was estimated using linear regression analysis. Statistical analysis was performed with Origin 5.0 software (OriginLab, Northampton, MA). The difference between the mean values of measured parameters was determined by the Student's *t*-test.

Real-Time Quantitative RT-PCR

Reverse transcription. Total cellular RNA was extracted using RNABle kit (Eurobio). RNA (10 μl) were reverse transcribed in a 25-μl reaction mixture consisting of first-strand buffer (25 mM Tris pH 8.3, 37.5 mM KCl, and 1.5 mM $MgCl_2$), 10 mM dithiothreitol, 1 mM each dNTP, 2.4 μg of random hexamers, 40 U RNase inhibitor (RNA guard; Amersham Biosciences), and 400 U MMLV reverse transcriptase (GIBCO-BRL). Reverse transcription was performed at 37°C for 60 min followed by 2 min at 100°C.

Quantitative PCR. For TRPC1, TRPC4, and TRPV2, quantitative (q)PCR was performed in the presence of 15 ng of cDNA and a 16-μl reaction mixture containing 10 μl Taqman Fast Universal Master Mix 2× (Applied Biosystems), 1 μl of Taqman Gene Expression Assays 20× and 5 μl of water. Amplification was performed at 95°C for 10 min, followed by 40 cycles at 95°C (3 s) and 60°C (30 s). Reactions were performed in MicroAmp optical 96-well reaction plates (Applied Biosystems) using a 7500HT Real-Time PCR system (Applied Biosystems). All measurements were normalized to GAPDH gene (endogenous control) to account for the variability in the initial concentration and quality of the total RNA. Taqman Gene Expression Assays FAM/MGB probes were purchased from Applied Biosystems (Hs99999905_m1-Human GAPDH, Hs00608195_m1-Human TRPC1, Hs00211805_m1-Human TRPC4 and Hs00901640_m1-Human TRPV2, and Hs0300473_m1-Human Orai1).

SYBR Green system (Applied Biosystems) was also used for STIM1 and α_1-syntrophin. All measurements were normalized to GAPDH as a reference (endogenous control) to account for the variability in the initial concentration and quality of the total RNA. qPCR was performed in the presence of 100 ng cDNA and 15-μl reaction mixture containing 7.5 μl SYBR Green mix 2× and 900 nM of each primer (sens and reverse). Amplification was performed at 50°C for 2 min, 95°C for 10 min, followed by 40 cycles at 95°C (15 s) and 60°C (1 min). Reactions were carried out as described above.

Primers were as follows: for STIM1, forward primer: 5′-GAC-TGA-CAG-GGA-CTG-TGC-TGA-AG-3′ and reverse primer: 5′-AAG-AGA-GGA-GGC-CCA-AAG-AG-3′; for α_1-syntrophin, forward primer: 5′-CAA-GAT-GCC-TAT-TCT-CAT-TTC-C-3′ and reverse primer: 5′-TCC-TTC-ATA-TAC-TTG-ACC-TCC-AG-3′; and for GAPDH, forward primer: 5′-CAA-TGC-CTC-CTG-CAC-CAC-3′ and reverse primer: 5′-CCT-GCT-TCA-CCA-CCT-TCT-TG-3′.

Data Analysis

For all cation influx recording results, bar graphs represent mean rates of fluorescence decrease induced by Mn^{2+} (expressed in %/min) ± SE. The difference between mean values of measured parameters was determined by Student's *t*-test and considered significant at $P < 0.001$. For RT-qPCR and Western blot analysis, all experiments were repeated three times with myotubes from different patients. Bar graphs of RT-qPCR represent the mean of triplicates from three different experiments. The difference between mean values of measured parameters was determined by one-way ANOVA analysis and considered significant at $F < 0.05$ (ns).

Patch-Clamp Experiments

The measurements were carried out at room temperature (≈22°C). Patch electrodes (3–5 MΩ) were pulled from borosilicate glass capillaries using a vertical micropipette puller (Narishige, Tokyo, Japan). Voltage-clamp experiments were performed using an Axopatch 200B amplifier with a CV 203BU headstage (Molecular Devices, CA). Voltage command pulses were generated by a personal computer equipped with an analog-digital converter (Digidata 1200; Molecular Devices) using pCLAMP software v8.0 (Molecular Devices). Currents were filtered at 2 kHz and digitized at 5 kHz. The digitized currents were stored on a computer for later offline analysis. Cell capacitance (277.19 ± 102.65 pF; $n = 4$) was measured by integrating the area under the capacitative transient elicited by 10-mV depolarizing steps from a holding potential of −20 mV. Before the experiments, cells were washed with a bath solution containing the following (in mM): 145 Na-methansulfonate, 10 CsCl, 10 $CaCl_2$, 1.2 $MgSO_4$, 10 HEPES, and 10 glucose (pH was adjusted to 7.4 with NaOH). The patch pipettes were filled with the following (mM): 145 Cs-methanesulfonate, 1 EGTA, 8 $MgCl_2$, and 10 HEPES (pH adjusted to 7.2 with CsOH). Calcium store depletion was recorded using a calcium-free perfusion containing the following (in mM): 145 Na-methansulfonate, 20 CsCl, 1.2 MgSO4, 10 HEPES, and 10 glucose (pH was adjusted to 7.4 with NaOH). Depletion protocol consisting of three times 1 min alternated application of free Ca^{2+} perfusion + 5 μM CPA + 10 mM caffeine and of free Ca^{2+} solution + 15 μM CPA. SOC currents were then generated by perfusion of the bath solution + 10 μM nifedipine. The THC-induced current was recorded after the perfusion of bath solution supplemented with 100 μM THC + 10 μM nifedipine. A −10-mV correction of the liquid junction potential between the patch pipette and the bath solutions was performed before experiments. After break-in, cells were held at 0 mV and stimulated with depolarizing voltage ramps from +80 mV to −140 mV within 1 s every 5 s. Data were analyzed using a combination of pCLAMP software v8.0 (Molecular Devices), Microsoft Excel, and SigmaPlot 8.0 (SPS, Chicago, IL).

RESULTS

Characterization of Cation Influx in Normal and DMD Primary Human Myotubes

This work was performed on human primary myotubes from normal patients or patients suffering from DMD. We first checked the expression of dystrophin in these human primary cultures: as

expected this protein is localized at the sarcolemma in normal cultures and is absent in DMD myotubes (Fig. 1*A*). Two different cation influxes were recorded in both types of myotube: first, basal calcium entry, a spontaneous influx that occurs subsequent to the addition of manganese ions in the extracellular medium (without depletion, Fig. 1*C*), and second, the cation entry subsequent to SR calcium store depletion (Fig. 1*D*).

Basal cation entry was recorded using the quenching of fura-2 fluorescence by manganese technique. The perfusion of Mn^{2+} solution generated a similar basal calcium entry in normal and in DMD human primary myotubes (7.95 ± 0.44%/min, $n = 36$, and 7.34 ± 0.23%/min, $n = 30$, respectively; Fig. 1*D*). This shows that regulation of basal calcium entry from the extracellular space is not impaired at this stage.

We also investigated the presence, of a calcium influx triggered by SR depletion. For that, SR calcium store were depleted by activation of RyR with caffeine and inhibition of sarco(endo)plasmic reticulum calcium ATPase (SERCA) with CPA. Depletion protocol consisted of three perfusions (1 min each) of 10 mM caffeine in calcium-free solution with 5 μM CPA alternating with three perfusions (1 min each) of calcium-free solution with CPA (Fig. 1*B*). Once the SR stores were depleted, Mn^{2+} solution was introduced into the extracellular medium and cation influx was recorded (Fig. 1*C*). This influx was almost two fold higher in DMD primary human myotubes compared with normal ones (28.40 ± 0.45%/min, $n = 95$, and 15.93 ± 0.32%/min, $n = 98$, respectively) (Fig. 1*D*). These results show an abnormal increase of calcium influx in DMD human myotubes after SR store depletion, suggesting that the regulation of external calcium uptake after this stimulation is mishandled in DMD human primary myotubes. This influx is consistent with the one previously described by our group in mouse cell lines SolD6 expressing minidystrophin (14.70 ± 0.4%/min, $n = 124$) and SolC1 dystrophin-deficient (28.10 ± 0.8%/min, $n = 115$; Ref. 50). Interestingly, we observed similar absolute values and levels of increase (2-fold) in mouse and human models.

Pharmacological Profile of Cation Influx Recorded After SR Store Depletion

A panel of cation and calcium channels inhibitors was introduced in the last CPA solution perfusion and after SR store depletion in the Mn^{2+} solution. The influx we recorded in normal and in DMD primary human myotubes was not affected by the voltage-gated channel inhibitor nifedipine (5 μM; 13.67 ± 1.39%/min, $n = 15$, vs. 15.93 ± 0.32%/min, $n = 98$, in control condition and 25.6 ± 1.19 vs. 28.40 ± 0.45%/min, $n = 95$, in

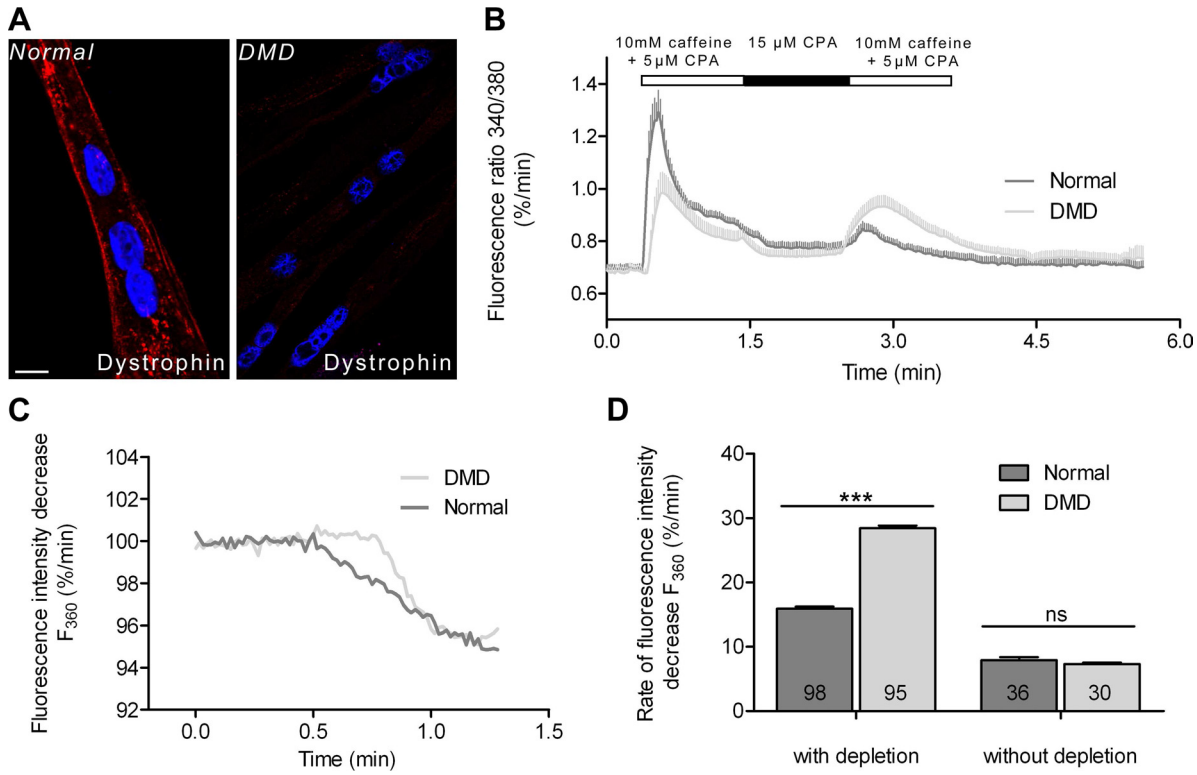

Fig. 1. Characterization of basal and sarcoplasmic reticulum (SR) store depletion-dependent cation influx in normal and Duchenne muscular dystrophy (DMD) primary human myotubes. *A*: immunostaining with anti-dystrophin antibody (in red) was performed in normal (*left*) and DMD human myotubes (*right*). DAPI staining (blue) was used to mark the nucleus. Images were obtained using confocal microscopy; bar = 10 μm. *B*: depletion of SR store protocol was constituted of 3 perfusions, 1 min each, of calcium-free solution containing 10 mM caffeine and 5 μM cyclopiazonic acid (CPA) alternated with 3 perfusions, 1 min each, of calcium-free solution containing 15 μM CPA. This protocol was applied similarly to normal (dark grey) and DMD (light grey) human myotubes. Cytosolic calcium variations were recorded by ratiometric measurement of fura 2 fluorescence intensity and shown as fluorescence ratios at 340 nm and 380 nm ± SE ($n = 12$). *C*: representative recording of fura 2 fluorescence during perfusion with 50 μM Mn^{2+} obtained from normal (dark grey) and DMD (light grey) human myotubes after application of the depletion protocol. *D*: manganese influx was recorded without or after SR calcium store depletion in normal and DMD primary human myotubes. Measurements are represented as slopes of the Mn^{2+}-induced decreasing phase of fura 2 fluorescence measured at 360 nm and expressed as percent decrease per minute. Bar-graphs represent mean rates of fluorescence decrease induced by Mn^{2+} (expressed in %/min) ± SE in normal (dark grey) and DMD (light grey) human myotubes. ***$P < 0.001$; ns, nonsignificant.

control condition, respectively; Fig. 2*A*). Nifedipine is known to selectively inhibit voltage-dependent L-type calcium channels at this concentration (21, 31). This allowed ruling out the participation of voltage-gated channels in the recorded influx.

Gd^{3+} and 2APB, two nonselective inhibitors of calcium channels, were also tested. Both inhibitors completely abolished the SR depletion-dependent part of the calcium influx in the same way in normal and DMD primary human myotubes (Fig. 2*B*). In the presence of 10 μM Gd^{3+} and 50 μM 2APB, cation entry recorded in normal myotubes was 5.14 ± 0.29%/min, $n = 20$, and 5.89 ± 0.73%/min, $n = 19$, respectively, and in DMD myotubes was 5.83 ± 0.93%/min $n = 11$ and 6.63 ± 0.97%/min, $n = 12$, respectively. Then, we tested SKF-96365, a nonselective SOCE inhibitor (11, 43), and YM-58483, characterized as a selective inhibitor of SOCE (20, 27, 65). Cation influx recorded in normal human myotubes was inhibited in the same way by 40 μM of SKF-96365 (introduced during perfusion as described above) and by incubation with 1 μM of YM-58483 during 45 min loading with fura 2 (6.27 ± 0.35%/min, $n = 17$, and 8.65 ± 0.35%/min, $n = 43$, respectively). Similarly cation influx in DMD myotubes was also decreased by SKF-96365 and YM-58483 (8.87 ± 0.51%/min, $n = 13$, and 8.81 ± 0.45%/min, $n = 22$, respectively) (Fig. 2*C*). All together these results suggest that cation entry recorded in normal and DMD human primary myotubes after SR store depletion displays the classical pharmacological profile of SOCE.

Interestingly, none of these inhibitors had an effect on basal influx recorded in the absence of depletion (Fig. 2*D*). Indeed, in normal and DMD human myotubes, in the presence of these inhibitors we noticed no significant variation compared with the control condition (Fig. 2*D*): nifedipine: 8.24 ± 0.46%/min, $n = 15$, and 8.47 ± 0.40%/min, $n = 20$, respectively; Gd^{3+}: 7.79 ± 0.29%/min, $n = 26$, and 8.39 ± 0.31%/min, $n = 28$, respectively; 2APB: 8.61 ± 0.22%/min, $n = 15$, and 7.99 ± 0.50%/min, $n = 14$, respectively; and SKF-96365: 7.92 ± 0.32%/min, $n = 21$, and 8.06 ± 0.37%/min, $n = 21$, respectively; vs. control condition: 7.95 ± 0.44%/min, $n = 36$, and 7.34 ± 0.23%/min, $n = 30$, respectively. This part of cation entry shows resistance toward all tested agents. Only store-operated part of the influx was affected.

Expression Profile and Localization of TRPC1, TRPC4, STIM1, and Orai1, the Major Actors of SOCE

Since SOCEs has been shown to be carried by Orai1 and TRPC channels under the control of STIM1 (51), we decided to study the localization and expression of these proteins in normal and DMD primary human myotubes. We first explored the regulation of the transcriptional level in both myotube types. Quantitative RT-PCR showed no significant difference in TRPC1, TRPC4, STIM1, and

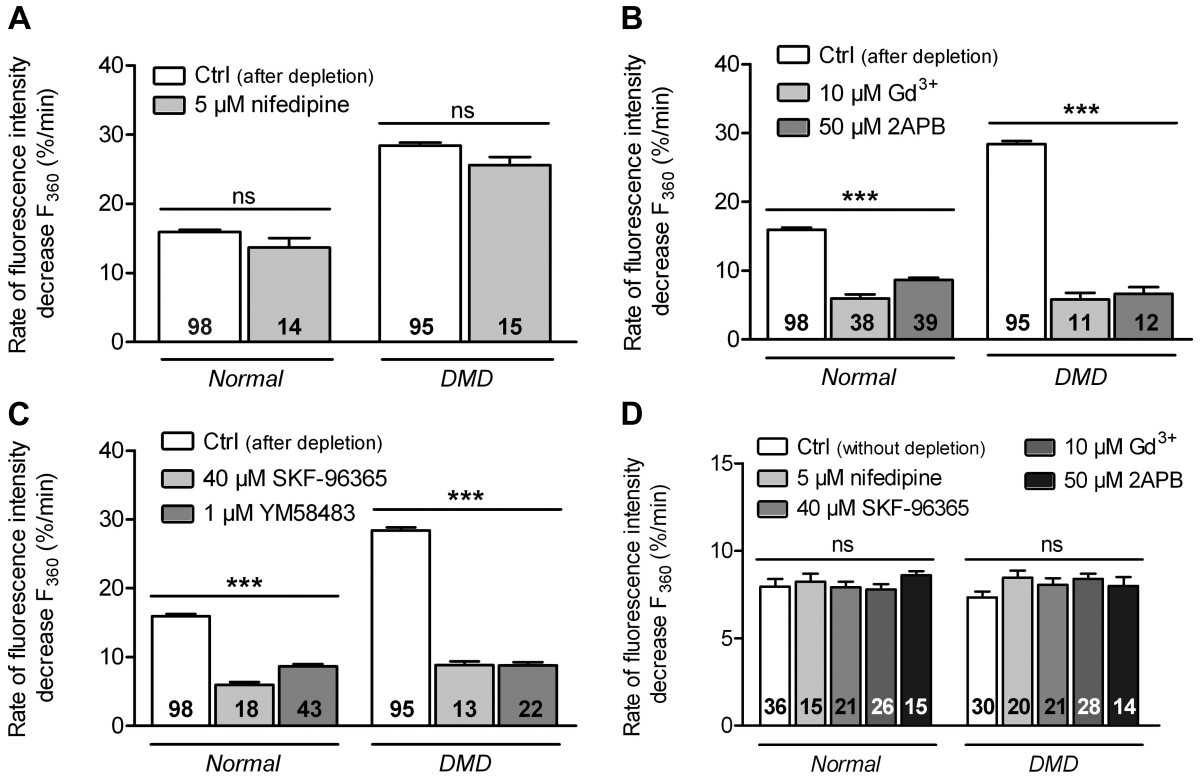

Fig. 2. Pharmacological profile of cation influx recorded in normal and DMD primary human myotubes. *A*: manganese influx was recorded in normal and DMD myotubes in the presence (light-grey columns) and absence (white columns) of 5 μM of the voltage-gated channel inhibitor nifedipine after SR calcium store depletion. *B*: nonselective calcium channel inhibitors Gd^{3+} (10 μM, light-grey columns) and 2-aminoethoxydiphenyl borate (2APB; 50 μM, dark-grey columns) were tested on normal and DMD human myotubes and compared with control condition (white columns) after SR store depletion. *C*: manganese influx triggered by SR store depletion was measured in the absence (white columns) or the presence of 40 μM SKF-96365, a nonselective store-operated calcium entry (SOCE) inhibitor (light-grey columns) or of 1 μM YM-58483, characterized as a selective inhibitor of SOCE (dark-grey columns). *D*: same pharmacological compounds were tested at the same concentrations on basal Manganese influx (without store depletion) and compared with control condition in normal and DMD human myotubes. ***$P < 0.001$.

Orai1 mRNA expression level between normal and DMD human myotubes (Fig. 3, A, *B*, *C*, and *D*, respectively). In both human myotube types, TRPC1 (Fig. 3*A*) showed mainly a sarcolemmal but also an internal localization that seem to be at the sarcoplasmic reticulum. Western blot analysis showed that TRPC1 protein was slightly decreased in DMD human myotubes. In the same manner we showed a strictly sarcolemmal localization of TRPC4 in normal and DMD myotubes with a decrease of the protein level in DMD human myotubes (Fig. 3*B*). Immunostaining with STIM1 antibody displayed a typical SR internal distribution in both myotube types and Western blot analysis revealed a slight increase of STIM1 expression in DMD human myotubes (Fig. 3*C*). Orai1 exhibited predominantly a sarcolemmal localization in both myotube types and a decrease of expression in DMD myotubes

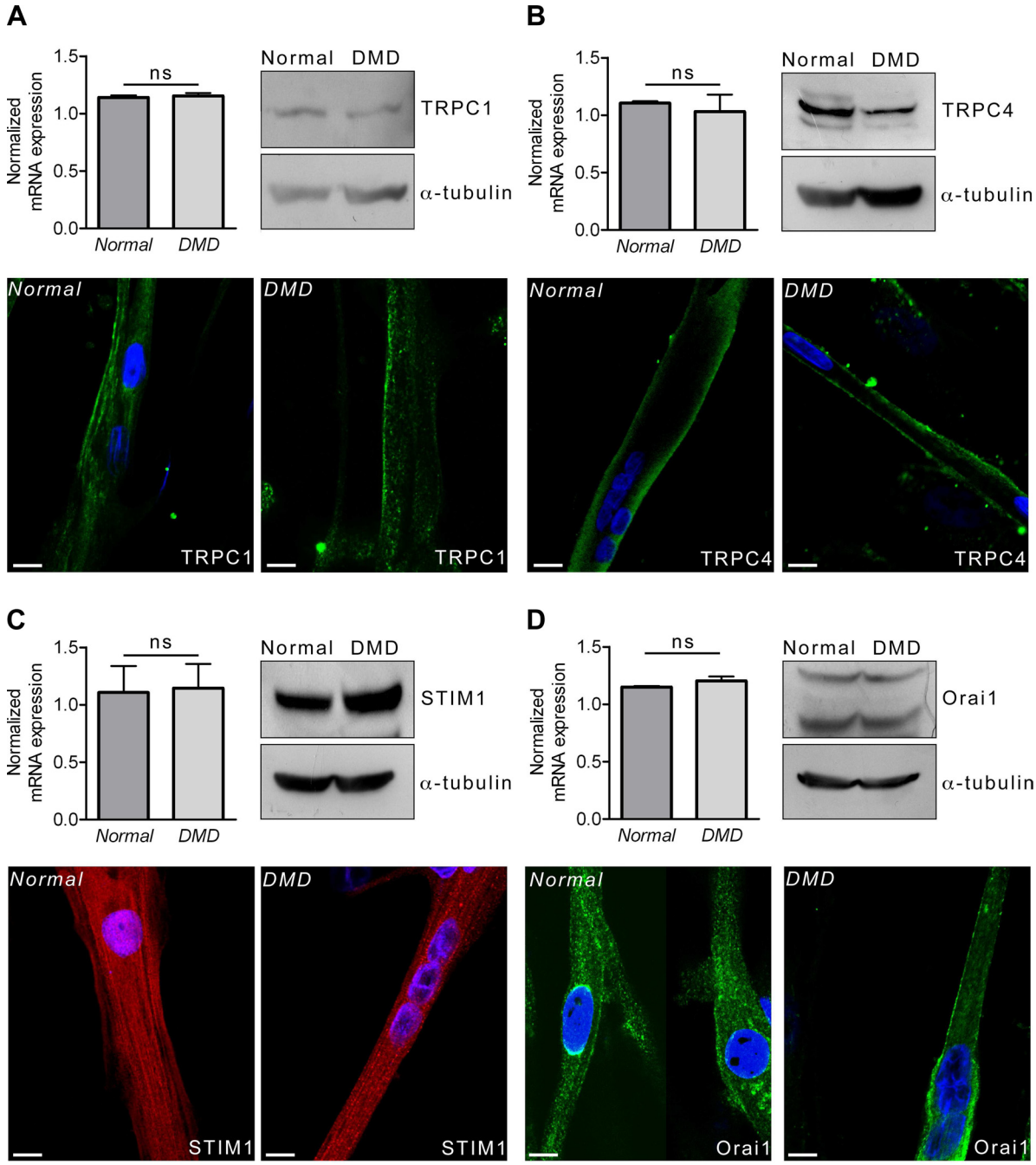

Fig. 3. Expression and localization of transient receptor potential channel TRPC1, TRPC4, stromal interaction molecule 1 (STIM1), and Orai1 in normal and DMD human myotubes. RT-quantitative (q)PCR, Western blot analysis, and immunofluorescence microscopy were performed on normal and DMD human myotubes after 11 days of differentiation to show localization, mRNA and protein expression of TRPC1 (*A*), TRPC4 (*B*), STIM1 (*C*), and Orai1 (*D*). The expression level of mRNA was addressed by quantitative RT-PCR-based analysis and GAPDH mRNA was used as an internal standard to normalize mRNA level. Expression level of each protein was analyzed by Western blot and compared with α-tubulin. Immunostaining experiments show the localization of TRPC1 (*A*), TRPC4 (*B*), STIM1 (*C*, in red), and Orai1 (*D*, in green). DAPI staining (blue) was used to mark the nucleus. Images were obtained using confocal microscopy; bar = 10 μm.

(Fig. 3*D*). Since mRNA expression levels are not different for TRPC1, TRPC4, and Orai1 between healthy and dystrophic myotubes, the decrease in channel protein amount is not due to a transcriptional regulation, but may be due to a lower stability of these channels.

α1-Syntrophin is Involved in the Abnormal Increase of SOCE in DMD Human Myotubes

α1-Syntrophin is a major partner of dystrophin glycoprotein complex that binds dystrophin through its syntrophin unique domain (1) and interacts with several ionic channels and signaling proteins using its PDZ (PSD-95, Discs-large, ZO-1) domain. We previously demonstrated a crucial role of α1-syntrophin and more precisely its PDZ domain in the regulation of SOCE in mouse myotubes (50, 59). This finding led us to seek the role of α1-syntrophin in the regulation of SOCE in the primary human myotubes.

We first checked the expression and localization of this protein in our models. We observed a slight decrease in α1-syntrophin expression in DMD human myotubes with a similar mRNA expression (Fig. 4*A*). The sarcolemmal localization of α1-syntrophin in normal human myotubes is lost to an intracellular one in DMD myotubes (Fig. 4*A*).

We also investigated the role of α1-syntrophin in the regulation of SOCE in human myotubes. Immunostaining shows that overexpression of α1-syntrophin in DMD myotubes allowed its readdressing to the subsarcolemma (Fig. 4*B*). We recorded SOCE in normal and DMD human myotubes after their transfections with FL α1-syn or α1-syntrophin without its PDZ domain (ΔN α1-syn). Transfection with full-length α1-syntrophin restored normal levels of SOCE in DMD human myotubes (15.02 ± 0.65%/min, $n = 20$) while the transfection with α1-syntrophin lacking its PDZ domain did not affect SOCE abnormal increase in DMD human myotubes (26.32 ± 1.25%/min, $n = 17$; Fig. 4*C*). Transfection of normal human myotubes with these two plasmids had no effect on SOCE (FL α1-syn: 14.90 ± 1.06%/min, $n = 10$; ΔN α1-syn: 12.90 ± 0.48%/min, $n = 11$; Fig. 4*C*). Transfection of EGFP (Pmax) as a negative control did not affect SOCE in normal: 15.37 ± 0.78%/min, $n = 17$, or in DMD: 26.88 ± 0.88%/min, $n = 14$.

SOCE Increase in DMD Primary Human Myotubes Depends on PLC and PKC

As we showed above (Fig. 1, *C* and *D*), SOCE is abnormally increased in DMD compared with normal primary human myotubes and this deregulation is dependent on α1-syntrophin (Fig. 4). To further understand the machinery leading to calcium mishandling in DMD human myotubes and since inositol 1,4,5-trisphosphate (the product of PLC catalytic activity) is increased in dystrophic human and murine cell lines (37), we investigated the PLC pathway as an underlying mechanism for this deregulation. PLC activity was blocked with a membrane-permeable PLC inhibitor, U73122. Several studies have previously shown that pretreatment with 5 or 10 μM U73122 prevented PLC activation fully and irreversibly (9, 30). Normal and DMD myotubes were incubated 15 min in the presence of 5 μM and 10 μM U73122 before SOCE recording. No significant changes have been observed in SOCE recorded in normal human myotubes after PLC inhibition (5 μM U73122: 14.76 ± 0.59%/min, $n = 29$; and 10 μM U73122: 14.18 ± 0.41%/min,

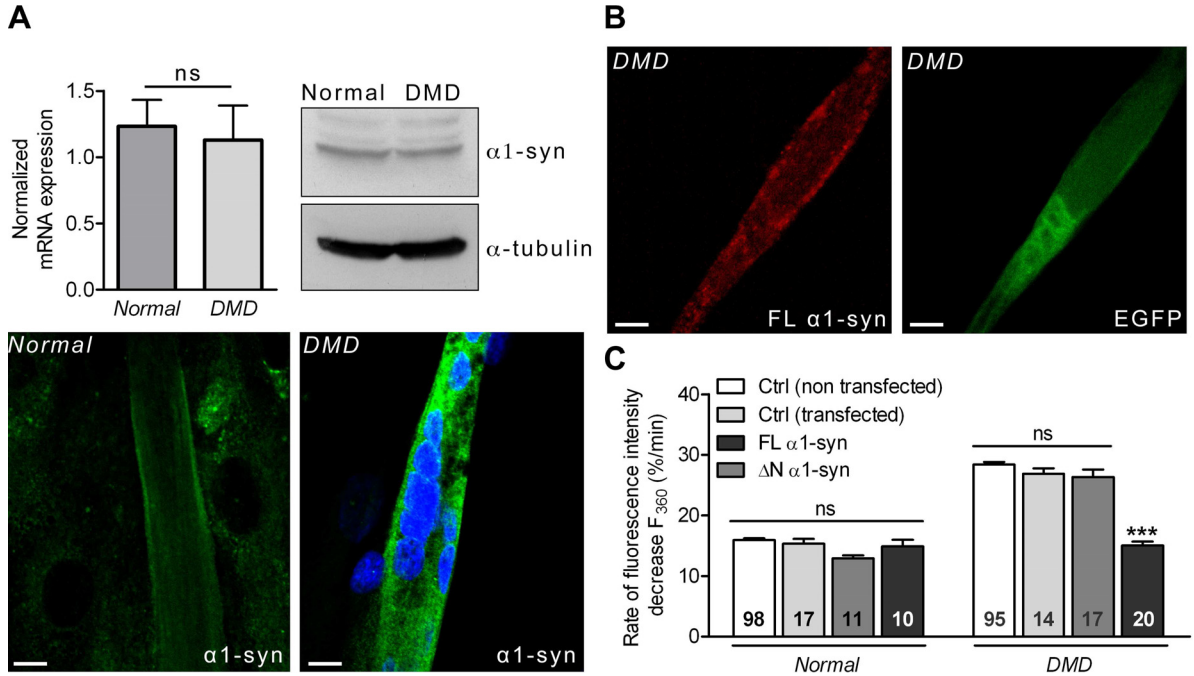

Fig. 4. Regulation of store-dependent cation entry by α1-syntrophin in primary human myotubes. *A*: RT-qPCR and Western blot analysis were used to compare mRNA and protein expression of α1-syntrophin between normal and DMD human myotubes. Immunostaining against α1-syntrophin (in green) shows its localization in normal (*left*) and DMD (*right*) human myotubes. DAPI staining (blue) was used to mark the nucleus in normal myotubes. Images were obtained using confocal microscopy; bar = 10 μm. *B*: immunostaining against α1-syntrophin was performed on DMD myotubes after transfection with full-length α1-syntrophin in red. Green staining (EGFP) allows the detection of transfected cells; bar = 20 μm. *C*: store-operated cation entry was recorded in normal and DMD human myotubes in control or transfected myotubes. Ctrl, Pmax; α1-syn, α1-syntrophin; FL α1-syn, full-length α1-syntrophin; ΔN α1-syn, PDZ domain deleted α1-syntrophin. ***$P < 0.001$.

$n = 36$; vs. control condition: 15.93 ± 0.32%/min, $n = 98$; Fig. 5*A*), suggesting that PLC is not involved in SOCE in normal myotubes. On the contrary, 5 and 10 μM of U73122 inhibited respectively 50% and 51% of SOCEs measured in DMD human myotubes (5 μM U73122: 14.17 ± 0.62%/min, $n = 42$; 10 μM U73122: 14.46 ± 0.69%/min, $n = 29$, vs. 28.40 ± 0.45%/min, $n = 95$ in control condition) while treatment with 10 μM U73343 an inactive analog of U73122 had no effect on SOCE in DMD myotubes (26.93 ± 0.73%/min, $n = 29$; Fig. 5*A*). The specific involvement of PLCβ$_1$ an essential isoform in skeletal muscle (16) was investigated by infecting DMD human myotubes with PLCβ$_1$ lentiviral particles or CopGFP control lentiviral particles. This resulted in a decrease of SOCE (shPLCβ1: 17.05 ± 0.85%/min, $n = 11$, and copGFP: 25.42 ± 1.12%/min, $n = 8$; Fig. 5*B*), equivalent to the inhibition obtained with pharmacological inhibitors. Therefore, PLC plays an important role in SOCE deregulation in DMD human myotubes given that the blockage of PLC restored SOCE at their normal levels.

Since PLC is known to stimulate PKC, we decided to look into the implication of this kinase in the deregulation of SOCE in DMD human myotubes. We used BIM, a highly selective, cell-permeable, and reversible PKC inhibitor shown to inhibit PKC at 1.5 μM (10). A 45-min preincubation of normal human myotubes with 1.5, 10, and 50 μM of BIM had no effect on SOCE (1.5 μM BIM: 13.54 ± 0.93%/min, $n = 32$; 10 μM BIM: 16.81 ± 0.48%/min, $n = 31$; and 50 μM 15.54 ± 0.38%/min, $n = 31$; vs. control condition: 15.93 ± 0.32%/min, $n = 98$; Fig. 5*C*). On the other hand, the inhibition of PKC in DMD myotubes with 1.5, 10 and 50 μM BIM decreased 56, 46, and 56% of SOCE respectively, (1.5 μM BIM: 12.34 ± 1.27%/min $n = 35$; 10 μM BIM: 15.39 ± 0.41%/min, $n = 54$; and 50 μM 12.49 ± 0.84%/min, $n = 17$; vs. control condition: 28.40 ± 0.45%/min, $n = 95$; Fig. 5*C*). PKC is thus implicated in SOCE deregulation in DMD human myotubes.

We also looked into the role of intracellular calcium in the activation of PKC and used TPEN, a low-affinity calcium chelator, to mime SR calcium store depletion without any calcium release in the cytoplasm (Fig. 5*D*). Depletion with TPEN allowed recovering normal levels of SOCE entry in DMD myotubes suggesting that cytoplasmic calcium concentration is involved in the abnormal increase of cation influx observed in DMD human myotubes. All together these results involve Ca^{2+}/PLC/PKC pathway in the elevated SOCE in DMD primary human myotubes.

Characterization of TRPV2-Dependent Calcium Influx in Normal and DMD Primary Human Myotubes

TRPV2 has been shown to play an important role in *mdx* fibers and seems to constitute a major input path of Ca^{2+} in

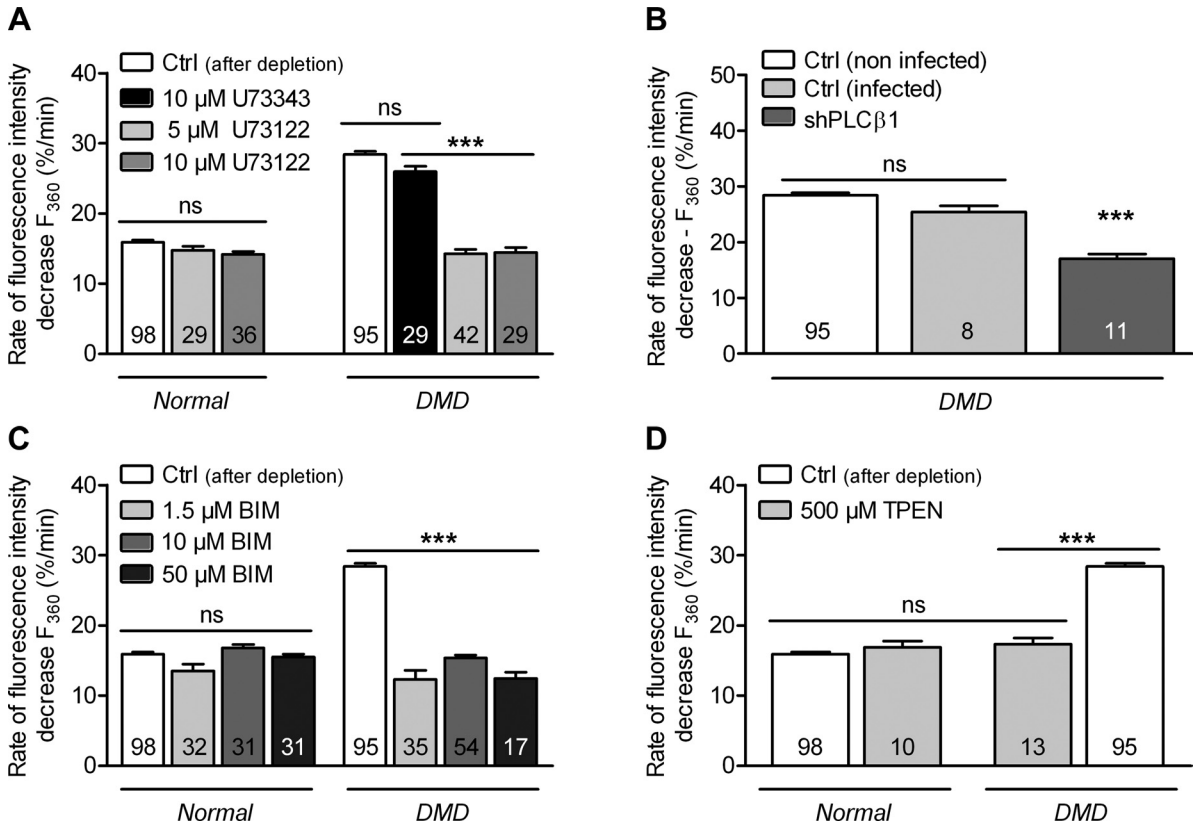

Fig. 5. Effect of U73122 and bisindolylmaleimide I (BIM) on SOCE in human myotubes. *A*: normal and DMD human myotubes were preincubated for 15 min with 5 μM (light-grey columns) and 10 μM (dark-grey columns) of PLC inhibitor U73122 before SOCE measurement and compared with control condition (white columns). Effect of 10 μM U73343, a U73122 inactive analog, was also tested in DMD myotubes (black column). *B*: DMD myotubes were infected with control copGFP (light-grey columns) or PLCβ$_1$ (dark-grey columns) lentiviral particles before SOCE measurement after caffeine + CPA depletion and compared with control condition (white columns). *C*: normal and DMD myotubes were incubated 45 min in the presence of 1.5, 10, and 50 μM of the selective PKC inhibitor BIM before SOCE measurement and compared with control condition. *D*: SOCE was recorded in normal and DMD myotubes after TPEN-dependent depletion. ***$P < 0.001$.

dystrophic muscle fibers (29, 64). Given the essential implication of TRPV2 shown in *mdx* and the protective effect of its downregulation, we considered studying TRPV2-dependent influx in normal and DMD primary human myotubes.

We studied the localization and the expression of TRPV2 in normal and DMD human myotubes (Fig. 6*A*). Immunostaining with antibody against TRPV2 presents an internal localization in both normal and DMD myotubes with a partial translocation to the plasma membrane observed only in DMD myotubes. Western blot analysis and quantitative RT-PCR showed no difference in TRPV2 mRNA or protein expression between normal and DMD human myotubes.

To study the physiological role of TRPV2 in human myotubes, we used THC, a well known activator of human and rat TRPV2 (45) and RR, an inhibitor of TRPV2 (36, 45). Calcium influx was recorded in normal and DMD human myotubes without depletion and only after the introduction in the extracellular medium of Mn^{2+} solution supplemented with 100 μM THC with or without 30 μM RR (Fig. 6, *C* and *D*). The activation with 100 μM THC causes an increase of cation influx in normal and DMD myotubes (19.08 ± 1.5%/min, n = 21, and 24.76 ± 1.09%/min, n = 32, respectively). This elevation was abolished in the presence of 30 μM RR in both myotube types (7.81 ± 0.36%/min, n = 26, and 8.45 ±

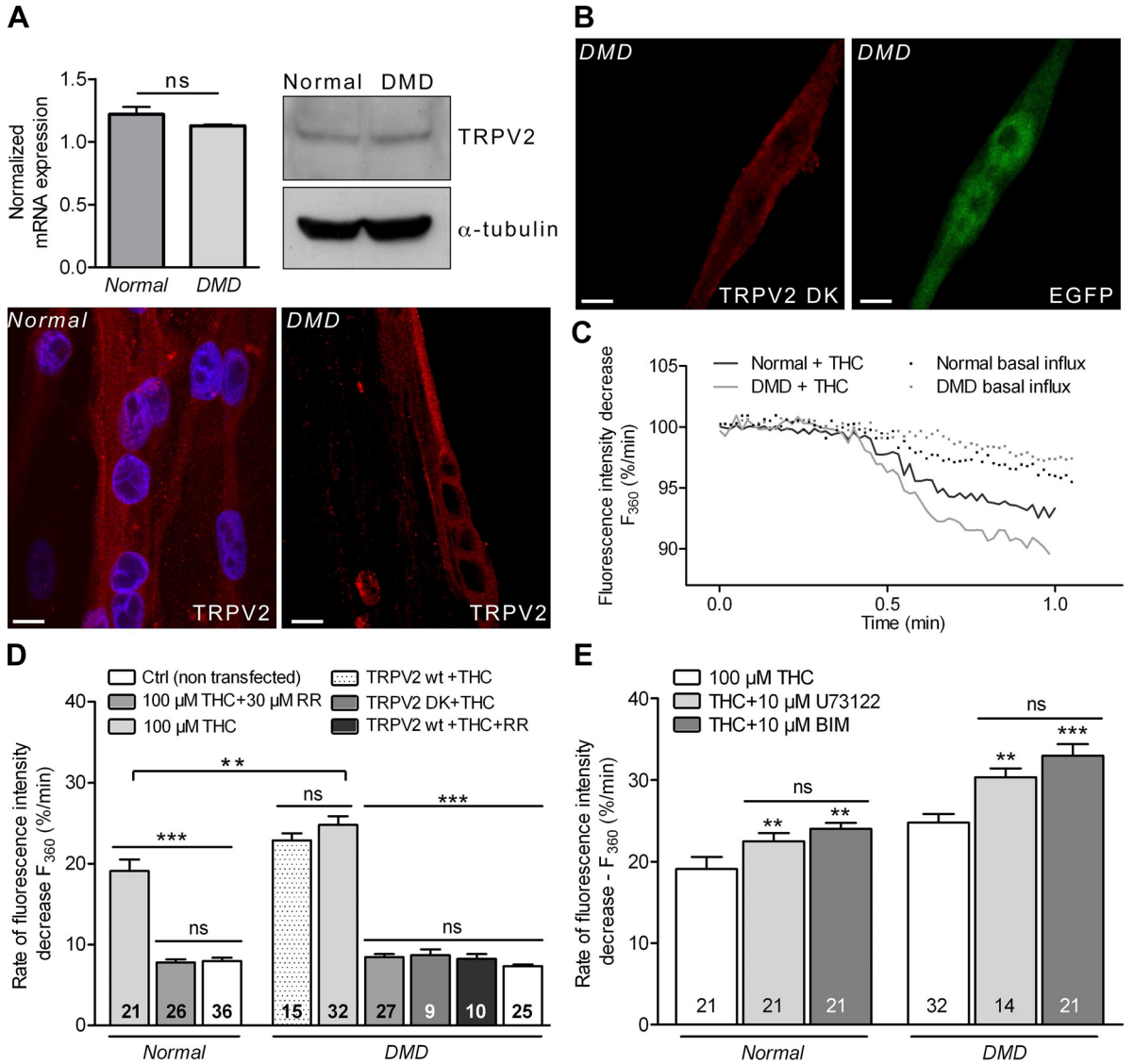

Fig. 6. TRP vanilloid 2 (TRPV2)-dependent cation influx in normal and DMD primary human myotubes. *A*: RT-qPCR and Western blot analysis were used to compare mRNA and protein expression of TRPV2 between normal and DMD human myotubes. Immunostaining against TRPV2 (in red) shows its localization in normal (*left*) and DMD (*right*) human myotubes. DAPI staining (blue) was used to mark the nucleus in normal myotubes. Images were obtained using confocal microscopy; bar = 10 μm. *B*: immunostaining against TRPV2 was performed on DMD myotubes after transfection with TRPV2 dominant-negative (DK) in red. The green staining (EGFP) allows the detection of transfected cells; bar = 20 μm. *C*: Representative manganese Influx recording without SR depletion in the presence or absence of Δ^9-Tetrahydrocannabinol (THC; TRPV2 activator) in normal and DMD myotubes. *D*: cation influx was recorded (without SR calcium store depletion) in the presence of 100 μM THC with or without 30 μM RR (TRPV2 inhibitor) in normal and DMD myotubes. DMD human myotubes were transfected with wild-type (WT) TRPV2 and TRPV2 dominant-negative DK. The consequence of these transfections has been studied without SR depletion in the presence of only Mn^{2+}, 100 μM THC or 100 μM THC + 30 μM RR. *E*: effect of U73122 and BIM on TRPV2-dependent calcium entry in human myotubes. Normal and DMD human myotubes were preincubated for 15 and 45 min with 10 μM U73122 (light-grey columns) and 10 μM BIM (dark-grey columns), respectively, before TRPV2-dependent calcium entry measurement and compared with control condition (white columns). $^{**}P < 0.05$; $^{***}P < 0.001$.

0.37%/min, $n = 27$, respectively). The fact that the increase of calcium influx observed in the presence of THC was eliminated by RR suggests that the recorded influx is TRPV2 dependent (Fig. 6*D*). To further confirm this proposal, we transfected DMD myotubes with pIRES2-AcGFP1 vector containing WT TRPV2 or TRPV2 DK and the cation influx was recorded 48 h after transfection. DMD myotubes transfected with TRPV2 DK exhibit a sarcolemmal expression of this dominant-negative showed by immunostaining experiments (Fig. 6*B*). The activation with 100 μM THC had no effect on cation influx in TRPV2 DK-transfected DMD myotubes (8.71 ± 0.68%/min, $n = 9$). The influx recorded in WT-transfected DMD myotubes in the presence of 100 μM THC and 30 μM RR was equivalent to that in the control condition with only Mn^{2+} stimulation (8.24 ± 0.58%/min, $n = 10$) and was not significantly different from the nontransfected myotubes in the presence of only 100 μM THC (22.90 ± 0.87%/min, $n = 15$; Fig. 6*D*). This demonstrates that the influx recorded in those specific conditions is carried by TRPV2. Interestingly, the influx measured after the activation of TRPV2 with 100 μM THC was significantly (95% confidence interval, $P < 0.05$, with Student *t*-test) more important in DMD primary human myotubes than in normal ones. Thus TRPV2 seems to be involved in calcium homeostasis impairment.

We also investigated the role of PLC and PKC in the abnormal increase of TRPV2-dependent calcium entry in these myotubes. Pharmacological inhibition of PLC (10 μM U73122) or PKC (10 μM BIM) was performed before the activation of TRPV2-dependent calcium entry using 100 μM THC. Interestingly we observed an increase of these entries in normal (Ctrl: 19.08 ± 1.46%/min, $n = 21$; BIM: 22.45 ± 0.99%/min, $n = 21$; and U73122: 24.02 ± 0.69%/min, $n = 21$) as well as in DMD myotubes (Ctrl: 24.76 ± 1.05%/min, $n = 32$; BIM: 30.35 ± 1.08%/min, $n = 14$; and U73122: 33.57 ± 1.39%/min, $n = 21$; Fig. 6*E*). This suggests that PLC/PKC pathway exerts the same regulatory effect on TRPV2 channels in normal and DMD myotubes and thus does not seem to be implicated in the enhancing of TRPV2-dependent calcium entry in DMD myotubes.

SOCE and THC-Induced Calcium Entry are Supported By Distinct Channels in Human Myotubes

To determine the connection between SOCE and THC-induced calcium entry two experiments were performed. First, SOCE was recorded in myotubes transfected with TRPV2 dominant-negative, DK, to achieve TRPV2 channels inhibition (Fig. 7*A*). No significant difference has been observed when compared with transfected control (Pmax) or nontransfected control in normal (Ctrl: 15.93 ± 0.32%/min, $n = 98$; Pmax: 15.51 ± 0.83%/min, $n = 15$; and DK: 14.62 ± 0.53%/min, $n = 15$) and DMD myotubes (Ctrl: 28.40 ± 0.45%/min, $n = 95$; Pmax: 27.93 ± 1.05%/min, $n = 12$; and DK: 27.37 ± 1.50%/min, $n = 14$; Fig. 7*A*). This suggests that TRPV2 channels are not involved in SOCE likely supported by Orai and TRPC channels as previously demonstrated in mouse myotubes (49). We also studied the effect of SOCE inhibition on TRPV2-dependent calcium entry in both cell types (Fig. 7*B*). One-hundred micromoles of THC were used to activate TRPV2 channels in the presence of 1 μM YM58483, SOCE blocker. The inhibition of SOCE had no significant effect on TRPV2-dependent calcium entry in normal (Ctrl: 19.08 ± 1.46%/min, $n = 21$; and 1 μM YM58483: 18.03 ± 0.78%/min, $n = 17$) and DMD myotubes (Ctrl: 24.76 ± 1.09%/min, $n = 32$; and 1 μM YM58483: 22.41 ± 1.09%/min, $n = 13$; Fig. 7*B*). We can thus conclude that SOCE and TRPV2-dependent calcium entry are supported by different channels in normal and DMD human myotubes. These channels do not seem to present any direct connection although both conduct abnormally high calcium entry in DMD cells. Whole cell patch-clamp experiments were performed in normal myotubes to characterize calcium current in response to caffeine + CPA perfusion (Fig. 7, *C* and *D*). The same experiments were done in normal myotubes to characterize calcium current in response to the calcium store depletion protocol already applied for measurements of cation entry with the fura-2 technique. The store depletion protocol consisted in perfusion of a 0 calcium solution with caffeine + CPA (Fig. 7, *C* and *D*). The perfusion of a 10 mM calcium solution after store depletion protocol activated a small inward current for negative membrane potentials. The current-voltage (*I*/*V*) curve obtained by the difference between ramp currents recorded in control and in 10 mM calcium perfusion displays a very small current density with an inward rectification representative of SOCE current.

Cation current was also recorded in response to THC perfusion in primary human normal myotubes during application of a voltage ramp (Fig. 7, *E* and *F*). Perfusion of THC activated a significant current at all potential. The resulting *I*/*V* curve is significantly different to the SOC *I*/*V* curve and close to the outwardly rectifying *I*/*V* curve obtained for TRPV2 expressed in Chinese hamster ovary cells (32). This confirms that caffeine + CPA perfusion and THC perfusion are stimulating different currents and activating independently SOCs and TRPV2, respectively.

DISCUSSION

Recent evidences have challenged the idea that Ca^{2+} entry contributes little to calcium homeostasis in skeletal muscle, and SOCE has been proposed to have critical influence in muscle development and disease (54). SOCE requires depletion of the internal stores and has been mainly characterized as a major calcium entry pathway in nonexcitable cells (47). It was also described in mouse myotubes (22), mouse fibers (35), and normal human myotubes by stimulating RyR resulting in the liberation of calcium from the SR to the cytoplasm (63). The present work confirms that cation influx can be evoked in human myotubes by the depletion of the SR calcium store using the stimulation of RyR with caffeine and the inhibition of calcium recapture by blocking SR SERCA pump using CPA (Fig. 1*B*).

Cation entry in response to the SR-depletion protocol in human myotubes showed the pharmacological profile previously reported for SOCE (Fig. 2), and the same profile has been noticed between DMD and normal ones. Measurements of cation entry showed an abnormal increase of store-operated cation entry in DMD primary human myotubes compared with normal ones. Indeed, SOCE was almost twofold higher in DMD primary human myotubes, suggesting that this abnormal cation entry may contribute to impairment of calcium homeostasis observed in DMD (Fig. 1*D*). This is consistent with the

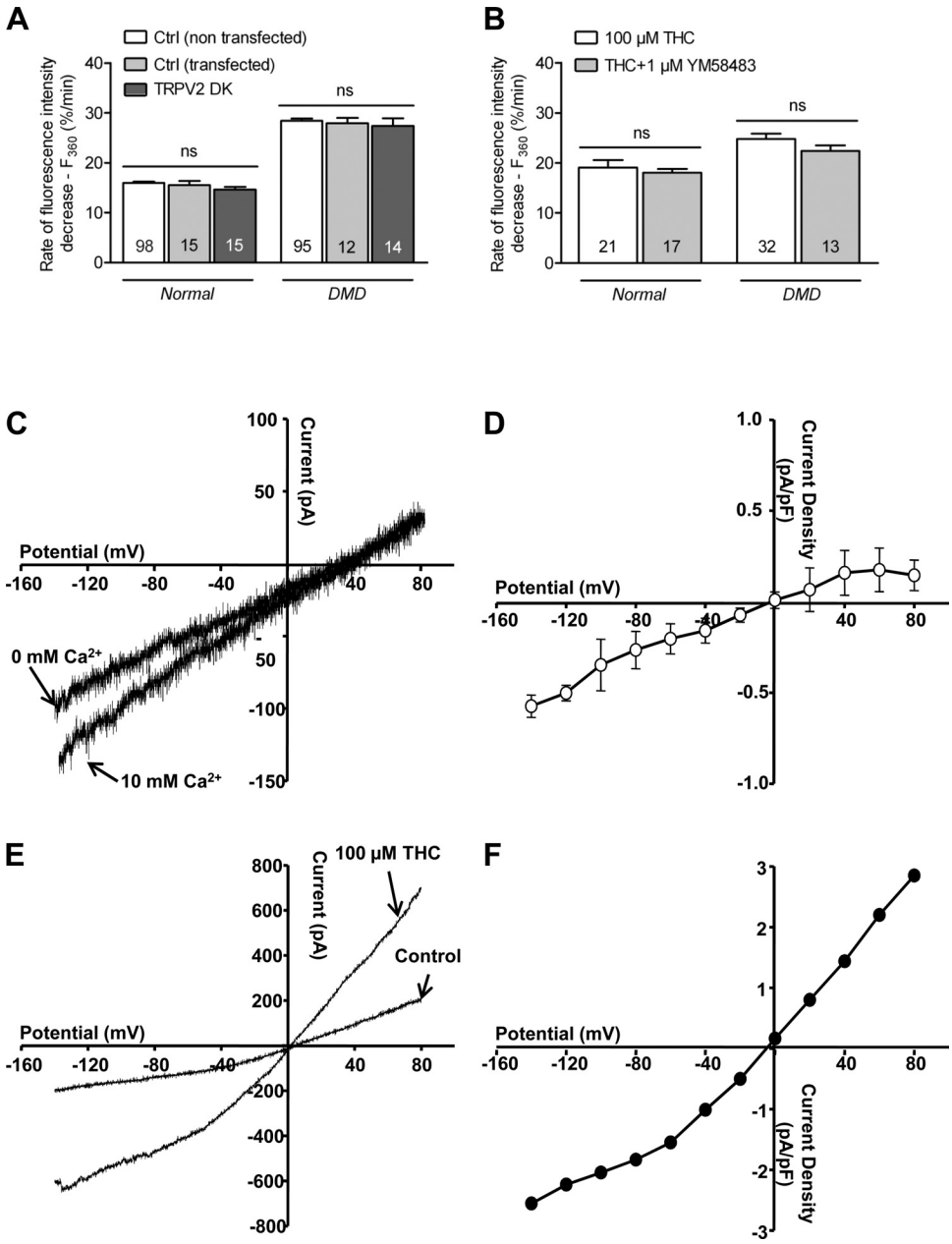

Fig. 7. Relation between SOCE and TRPV2 dependent cation entry in human myotubes. *A*: SOCE were recorded in normal and DMD human myotubes after transfection with Ctrl plasmid, Pmax (light-grey columns), or TRPV2 dominant-negative DK (dark-grey columns), SOCE measurement were compared with control condition (white columns). *B*: TRPV2-dependent cation entry was recorded in normal and DMD myotubes in the presence (light-grey columns) or the absence (white columns) of 1 μM YM58483 SOCE blocker. *C–F*: calcium currents recorded in primary human myotubes. *C*: representative ramp current traces recorded in the same cell in the absence (control) or in the presence of 10 mM calcium (SOC current) after calcium store depletion protocol. *D*: current-density-voltage relationship obtained from the difference between both control and SOC ramp currents in each cells ($n = 3$). *E*: ramp current traces recorded in the same cell with bath solution in the absence (control) or in the presence of 100 μM THC. *F*: current-density-voltage relationship obtained from the difference between both control and 100 μM THC ramp currents ($n = 1$).

differences of SOCE already reported between normal and dystrophin-deficient mouse myotubes and fibers (58, 59).

Early studies in murine model suggested the involvement of TRPC channels in SOCE (6), and our group showed previously the direct implication of TRPC1 and TRPC4 by selectively silencing their expression using small interfering RNA (50, 59). Moreover, overexpression of TRPC3 transgenic mice was sufficient to increase Ca^{2+} entry and to induce muscular dystrophy in vivo (42). The role of STIM1 and Orai1 has also been investigated in mouse models, and it is now acknowledged that these two proteins are key elements of SOCE in skeletal muscle. Indeed, it has been proved that STIM1-deficient mice show deficiency in SOCE accompanied by myopathies (53) and that the loss of expression of STIM1 or the expression of dominant-negative Orai1, E106Q, causes a significant decrease in SOCE in mouse myotubes (40). Since SOCE has been shown to involve the SR protein STIM1, and the sarcolemmal cation channels Orai1 and TRPCs, we looked for a differential expression of STIM1, Orai1, TRPC1, and TRPC4 proteins in normal and DMD primary human myotubes. Although we expected an increase in the expression of these proteins in DMD human myotubes, no noticeable difference was observed at the protein level after Western blot analysis. During primary culture of human myotubes, a change in expression of SOCE actors is thus not responsible for the enhancement of cation entry in DMD myotubes. Instead, we found that TRPC4, TRPC1, and Orai1 were less abundant in DMD human myotubes. Since mRNA expression levels are not different for TRPC1, TRPC4, and Orai1 between healthy and dystrophic myotubes, the decrease at the protein level may reflect an increase in protein degradation or a decrease of channels stability when not associated with the dystrophin

scaffold. This decrease in store-operated channels is, however, not accompanied by a decrease of SOCE, which is enhanced by PLC/PKC pathway. Only the STIM1 protein level was slightly elevated in these myotubes (Fig. 3). This is the first study of the expression of these proteins in human DMD myotubes. Only the mRNA levels of STIM1 and Orai1 were already compared with a microarray analysis of human skeletal muscle biopsies from control patients and DMD patients (Gene Expression Omnibus: http://www.ncbi.nlm.nih.gov/geo/). This study indicated that the STIM1 mRNA levels tended to decrease in the muscle of the dystrophic patients and that the Orai1 mRNA levels were not significantly changed (for review: see Ref. 34), which confirms our observations. This indicates a difference between the human and murine models since a dramatic increase of STIM1/Orai-protein level has been reported in *mdx* muscle fibers (15). Thus we showed the major SOCE actors were present in primary human myotubes but the role of STIM1, Orai1, and TRPC channels in the establishment of SOCE in this model needs to be investigated in a complementary study.

As we suggested before for mouse myotubes (50, 59), SOCE impairment is likely due to dysfunction in mechanisms of SOCE regulation. Furthermore, it has been shown that PLC/PKC pathway is involved in SOCE since the blocking of PLC or PKC completely abolished the thapsigargin-dependent calcium entry in endothelial cell line (3). We thus investigated the implication of PLC in SOCE impairment in DMD human myotubes and pointed the dependency of SOCE deregulation on this pathway using a specific pharmacological inhibitor U73122 (Fig. 5*A*). This inhibition had no effect in normal human myotubes as reported by Weigl et al. (63).

PLC can activate conventional PKC isoforms (α, β_1, β_2, and γ; Ref. 8), and, on the other hand, SOCE actors such as TRPC channels, Orai1, and STIM1 seem to be regulated by phosphorylation (2, 33, 36, 39, 46, 52). The PKC blocker, BIM restored SOCE to normal levels in DMD human myotubes and had no effect on SOCE in normal ones, suggesting that PKC are also involved in the deregulation of SOCE in DMD (Fig. 5*B*). It is well known that calcium ion is involved in conventional PKC isoforms pathway. In DMD human myotubes, depletion using TPEN induced a SOCE equivalent to that observed in normal human myotubes after caffeine/CPA-induced Ca^{2+} store depletion or after a TPEN-dependent depletion (Fig. 5*C*). We can thus draw a SOCE regulatory scheme involving Ca^{2+}/PLC/PKC pathway in DMD primary human myotubes.

To understand DMD calcium mishandling, several models of regulation have been suggested in mice. Our group proposed a regulation by α_1-syntrophin and showed the capacity of this protein to reestablish normal SOCE levels in dystrophin-deficient mouse myotubes (50, 59). Our observations confirm the delocalization of α_1-syntrophin to an internal sparse localization in DMD human myotubes comparing to the subsarcolemmal distribution in normal ones. Moreover, we showed that transfection of FL α_1-syn restores normal levels of SOCE in the absence of dystrophin and that its regulatory role is performed through its PDZ domain (Fig. 4*C*). These observations are consistent with the findings in murine myotubes and highlight the key role of α_1-syntrophin in the regulation of SOCE in primary human myotubes.

In the murine model, calcium mishandling has been related to other calcium entry pathway such as TRPV2 channels, which can be activated by membrane stretch (44). It is normally localized in intracellular membrane compartments but is translocated to the plasma membrane in dystrophic muscle fibers (28). Its specific inhibition appears to improve muscular dystrophy phenotype in *mdx* mice expressing a dominant-negative mutant of TRPV2 channel that reduces Ca^{2+} entry in muscle fibers (29, 64). It was also shown that the sensitivity to muscle stretch is mainly due to the abnormal localization in the plasma membrane or to the abnormal regulation of TRPV2 channels (64).

Our work in human cells showed a partial delocalization of TRPV2 to the plasma membrane (Fig. 6*A*) and an abnormal increase in cation entry triggered by THC in DMD myotubes compared with normal ones (Fig. 6*D*). Blockage by RR and by the expression of TRPV2 dominant-negative indicates that this cation entry is carried out by TRPV2 channels. This strengthens the idea that TRPV2 is responsible for an abnormally increased cation entry in DMD human myotubes as shown in *mdx* fibers (29, 64). We also observed that PLC and PKC play a regulatory role on TRPV2 channels activity in both healthy and DMD myotubes, suggesting that this pathway is not implicated in increased TRPV2-dependent calcium entry observed in DMD myotubes (Fig. 6*E*).

Even though TRPV2 and SOC are both involved in Ca^{2+} deregulation in DMD myotubes, no connection has been found between TRPV2-dependent calcium entry and SOCE in human myotubes. TRPV2 channels inhibition using dominant-negative DK had no effect on SOCE (Fig. 7*A*), and SOCE inhibition using YM58483 did not affect TRPV2-dependent calcium entry (Fig. 7*B*). Therefore, no direct relation seems to exist between these entries in normal as well as in DMD human myotubes.

All together these findings give, for the first time, important elements regarding calcium mishandling in a human primary model of DMD. In this work we showed an abnormal increase of SOCE in DMD human myotubes that is dependent on Ca^{2+}/PLC/PKC pathway and highlighted the regulation of SOCE by α_1-syntrophin via its PDZ domain. We also determined a role of TRPV2 in the calcium mishandling in DMD human myotubes. With these new basics, several therapeutic approaches could be envisaged. α_1-Syntrophin seems to be sufficient to regulate abnormal cation entry triggered by SR store depletion in the absence of dystrophin. As already experimented with utrophin, upregulation of α_1-syntrophin could be used for compensating the absence of dystrophin (55). Furthermore, α_1-syntrophin presents the advantage of being already expressed in DMD muscle cells, which excludes the risk of immune response in treated patients.

We also showed that TRPV2 activity is abnormally enhanced in DMD human myotubes and that TRPV2-dependent cation entry is restored by TRPV2 dominant negative. This same mutant reduced the progressive loss of force developed by *mdx* muscles and their sensitivity to eccentric contractions (64). The small size of the TRPV2 cDNA could facilitate its cloning in recombinant adeno-associated viruses (rAAV) for infection of DMD skeletal muscle cells with dominant-negative TRPV2. This work proposes new insights regarding calcium influx disorders in DMD myotubes and offers perspectives for DMD treatment.

ACKNOWLEDGMENTS

We kindly thank Dr. Y. Iwata for providing us with TRPV2 WT and DK plasmids; Dr. M. Solinas for supplying us with Δ^9-tetrahydrocannabinol, and J. Habrioux for technical assistance in designing figures. We also thank the members of the confocal microscopy platform ImageUP.

GRANTS

This work was supported by grants from the Centre National de la Recherche Scientifique, French Ministry of Research, and Association Française Contre les Myopathies. This work is part of the thesis project of R. Harisseh supported by a fellowship from the Association Française Contre les Myopathies whose generous support is gratefully acknowledged.

DISCLOSURES

No conflicts of interest, financial or otherwise, are declared by the author(s).

AUTHOR CONTRIBUTIONS

Author contributions: R.H., A.C., N.D., and B.C. conception and design of research; R.H., A.C., and C.M. performed experiments; R.H., C.M., and B.C. analyzed data; R.H. and B.C. interpreted results of experiments; R.H., A.C., C.M., N.D., and B.C. prepared figures; R.H. and B.C. drafted manuscript; N.D. and B.C. edited and revised manuscript; N.D. and B.C. approved final version of manuscript.

REFERENCES

1. **Adams ME, Dwyer TM, Dowler LL, White RA, Froehner SC.** Mouse alpha 1- and beta 2-syntrophin gene structure, chromosome localization, and homology with a discs large domain. *J Biol Chem* 270: 25859–25865, 1995.
2. **Albert AP, Large WA.** Store-operated Ca^{2+}-permeable nonselective cation channels in smooth muscle cells. *Cell Calcium* 33: 345–356, 2003.
3. **Antigny F, Jousset H, Konig S, Frieden M.** Thapsigargin activates Ca(2)+ entry both by store-dependent, STIM1/Orai1-mediated, and store-independent, TRPC3/PLC/PKC-mediated pathways in human endothelial cells. *Cell Calcium* 49: 115–127, 2011.
4. **Batchelor CL, Winder SJ.** Sparks, signals and shock absorbers: how dystrophin loss causes muscular dystrophy. *Trends Cell Biol* 16: 198–205, 2006.
5. **Berchtold MW, Brinkmeier H, Muntener M.** Calcium ion in skeletal muscle: its crucial role for muscle function, plasticity, and disease. *Physiol Rev* 80: 1215–1265, 2000.
6. **Birnbaumer L.** The TRPC class of ion channels: a critical review of their roles in slow, sustained increases in intracellular Ca(2+) concentrations. *Annu Rev Pharmacol Toxicol* 49: 395–426, 2009.
7. **Bodensteiner JB, Engel AG.** Intracellular calcium accumulation in Duchenne dystrophy and other myopathies: a study of 567,000 muscle fibers in 114 biopsies. *Neurology* 28: 439–446, 1978.
8. **Boni LT, Rando RR.** The nature of protein kinase C activation by physically defined phospholipid vesicles and diacylglycerols. *J Biol Chem* 260: 10819–10825, 1985.
9. **Broad LM, Braun FJ, Lievremont JP, Bird GS, Kurosaki T, Putney JW Jr.** Role of the phospholipase C-inositol 1,4,5-trisphosphate pathway in calcium release-activated calcium current and capacitative calcium entry. *J Biol Chem* 276: 15945–15952, 2001.
10. **Cardenas C, Muller M, Jaimovich E, Perez F, Buchuk D, Quest AF, Carrasco MA.** Depolarization of skeletal muscle cells induces phosphorylation of cAMP response element binding protein via calcium and protein kinase Calpha. *J Biol Chem* 279: 39122–39131, 2004.
11. **Clapham DE, Runnels LW, Strubing C.** The TRP ion channel family. *Nat Rev Neurosci* 2: 387–396, 2001.
12. **Deval E, Levitsky DO, Marchand E, Cantereau A, Raymond G, Cognard C.** Na(+)/Ca(2+) exchange in human myotubes: intracellular calcium rises in response to external sodium depletion are enhanced in DMD. *Neuromuscul Disord* 12: 665–673, 2002.
13. **Ducret T, Vandebrouck C, Cao ML, Lebacq J, Gailly P.** Functional role of store-operated and stretch-activated channels in murine adult skeletal muscle fibres. *J Physiol* 575: 913–924, 2006.
14. **Duke AM, Hopkins PM, Calaghan SC, Halsall JP, Steele DS.** Store-operated Ca^{2+} entry in malignant hyperthermia-susceptible human skeletal muscle. *J Biol Chem* 285: 25645–25653, 2010.
15. **Edwards JN, Murphy RM, Cully TR, von WF, Friedrich O, Launikonis BS.** Ultra-rapid activation and deactivation of store-operated Ca(2+) entry in skeletal muscle. *Cell Calcium* 47: 458–467, 2010.
16. **Faenza I, Bavelloni A, Fiume R, Santi P, Martelli AM, Maria BA, Lo V, V, Manzoli L, Cocco L.** Expression of phospholipase C beta family isoenzymes in C2C12 myoblasts during terminal differentiation. *J Cell Physiol* 200: 291–296, 2004.
17. **Fong PY, Turner PR, Denetclaw WF, Steinhardt RA.** Increased activity of calcium leak channels in myotubes of Duchenne human and mdx mouse origin. *Science* 250: 673–676, 1990.
18. **Franco A Jr, Lansman JB.** Stretch-sensitive channels in developing muscle cells from a mouse cell line. *J Physiol* 427: 361–380, 1990.
19. **Franco-Obregon A, Lansman JB.** Changes in mechanosensitive channel gating following mechanical stimulation in skeletal muscle myotubes from the mdx mouse. *J Physiol* 539: 391–407, 2002.
20. **He LP, Hewavitharana T, Soboloff J, Spassova MA, Gill DL.** A functional link between store-operated and TRPC channels revealed by the 3,5-bis(trifluoromethyl)pyrazole derivative, BTP2. *J Biol Chem* 280: 10997–11006, 2005.
21. **Helton TD, Xu W, Lipscombe D.** Neuronal L-type calcium channels open quickly and are inhibited slowly. *J Neurosci* 25: 10247–10251, 2005.
22. **Hopf FW, Reddy P, Hong J, Steinhardt RA.** A capacitative calcium current in cultured skeletal muscle cells is mediated by the calcium-specific leak channel and inhibited by dihydropyridine compounds. *J Biol Chem* 271: 22358–22367, 1996.
23. **Hopf FW, Turner PR, Denetclaw WF Jr, Reddy P, Steinhardt RA.** A critical evaluation of resting intracellular free calcium regulation in dystrophic mdx muscle. *Am J Physiol Cell Physiol* 271: C1325–C1339, 1996.
24. **Imbert N, Cognard C, Duport G, Guillou C, Raymond G.** Abnormal calcium homeostasis in Duchenne muscular dystrophy myotubes contracting in vitro. *Cell Calcium* 18: 177–186, 1995.
25. **Imbert N, Vandebrouck C, Constantin B, Duport G, Guillou C, Cognard C, Raymond G.** Hypoosmotic shocks induce elevation of resting calcium level in Duchenne muscular dystrophy myotubes contracting in vitro. *Neuromuscul Disord* 6: 351–360, 1996.
26. **Imbert N, Vandebrouck C, Duport G, Raymond G, Hassoni AA, Constantin B, Cullen MJ, Cognard C.** Calcium currents and transients in co-cultured contracting normal and Duchenne muscular dystrophy human myotubes. *J Physiol* 534: 343–355, 2001.
27. **Ishikawa J, Ohga K, Yoshino T, Takezawa R, Ichikawa A, Kubota H, Yamada T.** A pyrazole derivative, YM-58483, potently inhibits store-operated sustained Ca^{2+} influx and IL-2 production in T lymphocytes. *J Immunol* 170: 4441–4449, 2003.
28. **Iwata Y, Katanosaka Y, Arai Y, Komamura K, Miyatake K, Shigekawa M.** A novel mechanism of myocyte degeneration involving the Ca^{2+}-permeable growth factor-regulated channel. *J Cell Biol* 161: 957–967, 2003.
29. **Iwata Y, Katanosaka Y, Arai Y, Shigekawa M, Wakabayashi S.** Dominant-negative inhibition of Ca^{2+} influx via TRPV2 ameliorates muscular dystrophy in animal models. *Hum Mol Genet* 18: 824–834, 2009.
30. **Jin W, Lo TM, Loh HH, Thayer SA.** U73122 inhibits phospholipase C-dependent calcium mobilization in neuronal cells. *Brain Res* 642: 237–243, 1994.
31. **Kanwar U, Anand RJ, Sanyal SN.** The effect of nifedipine, a calcium channel blocker, on human spermatozoal functions. *Contraception* 48: 453–470, 1993.
32. **Kanzaki M, Zhang YQ, Mashima H, Li L, Shibata H, Kojima I.** Translocation of a calcium-permeable cation channel induced by insulin-like growth factor-I. *Nat Cell Biol* 1: 165–170, 1999.
33. **Kawasaki T, Ueyama T, Lange I, Feske S, Saito N.** Protein kinase C-induced phosphorylation of Orai1 regulates the intracellular Ca^{2+} level via the store-operated Ca^{2+} channel. *J Biol Chem* 285: 25720–25730, 2010.
34. **Kiviluoto S, Decuypere JP, De SH, Missiaen L, Parys JB, Bultynck G.** STIM1 as a key regulator for Ca^{2+} homeostasis in skeletal-muscle development and function. *Skelet Muscle* 1: 16, 2011.
35. **Kurebayashi N, Ogawa Y.** Depletion of Ca^{2+} in the sarcoplasmic reticulum stimulates Ca^{2+} entry into mouse skeletal muscle fibres. *J Physiol* 533: 185–199, 2001.
36. **Leffler A, Linte RM, Nau C, Reeh P, Babes A.** A high-threshold heat-activated channel in cultured rat dorsal root ganglion neurons resembles TRPV2 and is blocked by gadolinium. *Eur J Neurosci* 26: 12–22, 2007.

37. **Liberona JL, Powell JA, Shenoi S, Petherbridge L, Caviedes R, Jaimovich E.** Differences in both inositol 1,4,5-trisphosphate mass and inositol 1,4,5-trisphosphate receptors between normal and dystrophic skeletal muscle cell lines. *Muscle Nerve* 21: 902–909, 1998.
38. **Liou J, Kim ML, Heo WD, Jones JT, Myers JW, Ferrell JE Jr, Meyer T.** STIM is a Ca^{2+} sensor essential for Ca^{2+}-store-depletion-triggered Ca^{2+} influx. *Curr Biol* 15: 1235–1241, 2005.
39. **Lopez E, Jardin I, Berna-Erro A, Bermejo N, Salido GM, Sage SO, Rosado JA, Redondo PC.** STIM1 tyrosine-phosphorylation is required for STIM1-Orai1 association in human platelets. *Cell Signal* 24: 1315–1322, 2012.
40. **Lyfenko AD, Dirksen RT.** Differential dependence of store-operated and excitation-coupled Ca^{2+} entry in skeletal muscle on STIM1 and Orai1. *J Physiol* 586: 4815–4824, 2008.
41. **Marchand E, Constantin B, Balghi H, Claudepierre MC, Cantereau A, Magaud C, Mouzou A, Raymond G, Braun S, Cognard C.** Improvement of calcium handling and changes in calcium-release properties after mini- or full-length dystrophin forced expression in cultured skeletal myotubes. *Exp Cell Res* 297: 363–379, 2004.
42. **Millay DP, Goonasekera SA, Sargent MA, Maillet M, Aronow BJ, Molkentin JD.** Calcium influx is sufficient to induce muscular dystrophy through a TRPC-dependent mechanism. *Proc Natl Acad Sci USA* 106: 19023–19028, 2009.
43. **Moran MM, Xu H, Clapham DE.** TRP ion channels in the nervous system. *Curr Opin Neurobiol* 14: 362–369, 2004.
44. **Muraki K, Iwata Y, Katanosaka Y, Ito T, Ohya S, Shigekawa M, Imaizumi Y.** TRPV2 is a component of osmotically sensitive cation channels in murine aortic myocytes. *Circ Res* 93: 829–838, 2003.
45. **Neeper MP, Liu Y, Hutchinson TL, Wang Y, Flores CM, Qin N.** Activation properties of heterologously expressed mammalian TRPV2: evidence for species dependence. *J Biol Chem* 282: 15894–15902, 2007.
46. **Pozo-Guisado E, Campbell DG, Deak M, varez-Barrientos A, Morrice NA, Alvarez IS, Alessi DR, Martin-Romero FJ.** Phosphorylation of STIM1 at ERK1/2 target sites modulates store-operated calcium entry. *J Cell Sci* 123: 3084–3093, 2010.
47. **Putney JW Jr.** Capacitative calcium entry revisited. *Cell Calcium* 11: 611–624, 1990.
48. **Roos J, DiGregorio PJ, Yeromin AV, Ohlsen K, Lioudyno M, Zhang S, Safrina O, Kozak JA, Wagner SL, Cahalan MD, Velicelebi G, Stauderman KA.** STIM1, an essential and conserved component of store-operated Ca^{2+} channel function. *J Cell Biol* 169: 435–445, 2005.
49. **Sabourin J, Harisseh R, Harnois T, Magaud C, Bourmeyster N, Deliot N, Constantin B.** Dystrophin/alpha1-syntrophin scaffold regulated PLC/PKC-dependent store-operated calcium entry in myotubes. *Cell Calcium* 52: 445–456, 2012.
50. **Sabourin J, Lamiche C, Vandebrouck A, Magaud C, Rivet J, Cognard C, Bourmeyster N, Constantin B.** Regulation of TRPC1 and TRPC4 cation channels requires an alpha1-syntrophin-dependent complex in skeletal mouse myotubes. *J Biol Chem* 284: 36248–36261, 2009.
51. **Salido GM, Jardin I, Rosado JA.** The TRPC ion channels: association with Orai1 and STIM1 proteins and participation in capacitative and non-capacitative calcium entry. *Adv Exp Med Biol* 704: 413–433, 2011.
52. **Smyth JT, Petranka JG, Boyles RR, Dehaven WI, Fukushima M, Johnson KL, Williams JG, Putney JW Jr.** Phosphorylation of STIM1 underlies suppression of store-operated calcium entry during mitosis. *Nat Cell Biol* 11: 1465–1472, 2009.
53. **Stiber J, Hawkins A, Zhang ZS, Wang S, Burch J, Graham V, Ward CC, Seth M, Finch E, Malouf N, Williams RS, Eu JP, Rosenberg P.** STIM1 signalling controls store-operated calcium entry required for development and contractile function in skeletal muscle. *Nat Cell Biol* 10: 688–697, 2008.
54. **Stiber JA, Rosenberg PB.** The role of store-operated calcium influx in skeletal muscle signaling. *Cell Calcium* 49: 341–349, 2011.
55. **Tinsley JM, Fairclough RJ, Storer R, Wilkes FJ, Potter AC, Squire SE, Powell DS, Cozzoli A, Capogrosso RF, Lambert A, Wilson FX, Wren SP, De LA, Davies KE.** Daily treatment with SMTC1100, a novel small molecule utrophin upregulator, dramatically reduces the dystrophic symptoms in the mdx mouse. *PLos One* 6: e19189, 2011.
56. **Turner PR, Fong PY, Denetclaw WF, Steinhardt RA.** Increased calcium influx in dystrophic muscle. *J Cell Biol* 115: 1701–1712, 1991.
57. **Tyler KL.** Origins and early descriptions of "Duchenne muscular dystrophy". *Muscle Nerve* 28: 402–422, 2003.
58. **Vandebrouck A, Ducret T, Basset O, Sebille S, Raymond G, Ruegg U, Gailly P, Cognard C, Constantin B.** Regulation of store-operated calcium entries and mitochondrial uptake by minidystrophin expression in cultured myotubes. *FASEB J* 20: 136–138, 2006.
59. **Vandebrouck A, Sabourin J, Rivet J, Balghi H, Sebille S, Kitzis A, Raymond G, Cognard C, Bourmeyster N, Constantin B.** Regulation of capacitative calcium entries by alpha1-syntrophin: association of TRPC1 with dystrophin complex and the PDZ domain of alpha1-syntrophin. *FASEB J* 21: 608–617, 2007.
60. **Vandebrouck C, Duport G, Cognard C, Raymond G.** Cationic channels in normal and dystrophic human myotubes. *Neuromuscul Disord* 11: 72–79, 2001.
61. **Vandebrouck C, Martin D, Colson-Van SM, Debaix H, Gailly P.** Involvement of TRPC in the abnormal calcium influx observed in dystrophic (mdx) mouse skeletal muscle fibers. *J Cell Biol* 158: 1089–1096, 2002.
62. **Vig M, Beck A, Billingsley JM, Lis A, Parvez S, Peinelt C, Koomoa DL, Soboloff J, Gill DL, Fleig A, Kinet JP, Penner R.** CRACM1 multimers form the ion-selective pore of the CRAC channel. *Curr Biol* 16: 2073–2079, 2006.
63. **Weigl L, Zidar A, Gscheidlinger R, Karel A, Hohenegger M.** Store operated Ca^{2+} influx by selective depletion of ryanodine sensitive Ca^{2+} pools in primary human skeletal muscle cells. *Naunyn Schmiedebergs Arch Pharmacol* 367: 353–363, 2003.
64. **Zanou N, Iwata Y, Schakman O, Lebacq J, Wakabayashi S, Gailly P.** Essential role of TRPV2 ion channel in the sensitivity of dystrophic muscle to eccentric contractions. *FEBS Lett* 583: 3600–3604, 2009.
65. **Zitt C, Strauss B, Schwarz EC, Spaeth N, Rast G, Hatzelmann A, Hoth M.** Potent inhibition of Ca^{2+} release-activated Ca^{2+} channels and T-lymphocyte activation by the pyrazole derivative BTP2. *J Biol Chem* 279: 12427–12437, 2004.